JSAE 20159383
SAE 2015-01-1956

2-Butanone Laminar Burning Velocities – Experimental and Kinetic Modelling Study

Joachim Beeckmann, Raik Hesse, Liming Cai, Heinz Pitsch
Institute for Combustion Technology, RWTH Aachen University, Germany

Alexander Heufer
Physico-Chemical Fundamentals of Combustion, RWTH Aachen University, Germany

Yanmei Yang
Department of Thermal Engineering, Tsinghua University, China

ABSTRACT

2-Butanone (C_4H_8O) is a promising alternative fuel candidate as a pure as well as a blend component for substitution in standard gasoline fuels. It can be produced by the dehydrogenation of 2-butanol. To describe 2-butanone's basic combustion behaviour, it is important to investigate key physical properties such as the laminar burning velocity. The laminar burning velocity serves on the one hand side as a parameter to validate detailed chemical kinetic models. On the other hand, especially for engine simulations, various combustion models have been introduced, which rely on the laminar burning velocity as the physical quantity describing the progress of chemical reactions, diffusion, and heat conduction. Hence, well validated models for the prediction of laminar burning velocities are needed. New experimental laminar burning velocity data, acquired in a high pressure spherical combustion vessel, are presented for 1 atm and 5 bar at temperatures of 373 K and 423 K. An already existing mechanism, thoroughly validated with shock tube and rapid compression machine data, is compared against the new experimental data. It was found that the mechanism needs improvement with respect to correctly predicting temperature and pressure sensitivity. In addition, a linear and a non-linear post-processing technique are used to estimate the laminar flame speed in the burnt. Depending on the experimental conditions, such as temperature, pressure, and equivalence ratio, the extrapolation methods significantly differ in results. Thus, it has to be carefully assessed which extrapolation technique is the correct choice.

INTRODUCTION

Improving vehicle fuel economy while complying with emissions regulations is an important aspect of engine research. In order to achieve these improvements, it is a significant task to understand the complex technical combustion processes involved in the engine. Computer-based modelling is an important tool to analyse these combustion processes. In this context, the laminar burning velocity is one key parameter for the numerical simulation of gasoline engine combustion processes. Dependent only on the mixture composition, temperature, and pressure, it serves as a fundamental property of a fuel. This makes the laminar burning velocity an important global kinetic parameter for assessing fuel reactivity and for validating chemical kinetic mechanisms. Thus, for fuel components and fuel surrogates it is mandatory to know this quantity. In the past, the laminar burning velocity has been investigated mainly at atmospheric pressure, and as a consequence, experimental data for high pressure are sparse.

In this study, laminar burning velocities are investigated at ambient and increased pressures in a spherical combustion chamber with optical access. 2-butanone (C_4H_8O) has been chosen as a fuel for the measurements. It is a promising alternative fuel component which can be used as a pure as well as a blend component for substitution in standard gasoline fuels [1].One production pathway is the dehydrogenation of 2-butanol. New experimental laminar burning velocity data are presented for 1 atm and 5 bar at temperatures of 373 K and 423 K. The experimental data are obtained by applying a linear as well as a non-linear extrapolation technique, which are both assessed carefully.

Thereafter, results from an existing chemical mechanism are compared to the experimental data.

EXPERIMENTAL SETUP AND CONDITIONS

Experiments were performed using the closed vessel method combined with an optical Schlieren cinematography setup in order to acquire burning velocities at elevated pressures and temperatures. The experimental setup is shown schematically in Figure 1. The internal shape of the pressure vessel is spherical with an inner diameter of 100 mm; quartz windows with a diameter of 50mm are positioned on opposite sides [2].The outward location of the propagating flame is imaged using a dual-field-lens Schlieren arrangement [3]. It is combined with a high-speed CMOS camera (LaVision High-SpeedStar 6). Images were taken with 25000 frames per second (fps), at 448x448 pixels, and a resolution of 10.29 pixel/mm. The Schlieren system consists of a pulsed high power LED as a light source and an adjustable power output. The LED, type Luminus CBT-120-G-C11-CJ-G6 [4], emits green light between 530-535 nm. Optical lenses are an aspheric condenser lens and three spherical lenses. Two pinholes with a diameter of 0.5 mm are used and overexposure of the camera from flame radiation is prevented by an optical filter.

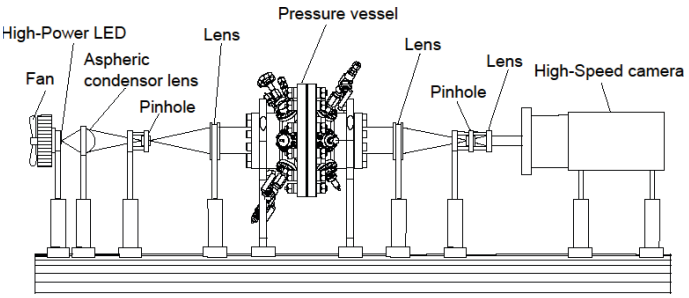

Figure 1 Schematic of the experimental setup

An external mixing vessel, directly connected to the combustion chamber via pipes, is employed for an external preparation of the air / fuel mixture. The fuel storage, the external mixing vessel, and all pipes in contact with fuel are heated to prevent fuel condensation. The amount of fuel needed can be calculated as a function of Φ, T, and p. The partial pressure method can be used for accurately measuring and controlling the filling process. In addition, a real gas correction has been applied by using the Soave modification of the Redlich-Kwong equation of state [5].

Before sparking, the heaters are turned off and the mixture is allowed to settle. A high voltage coil discharge is used for igniting the mixture at the midpoint of the vessel with extended spark plug electrodes of 1 mm diameter.

The present experimental setup was verified against methane / air and ethanol / air laminar burning velocities at various pressures, temperatures, and equivalence ratios [2, 6].

Experimental conditions were set up with compressed air, which consists of 20.94% oxygen, 78.13% nitrogen, and 0.93% argon. The basic physical properties of 2-butanone are listed in Table 1. Listed research octane (RON) and motor octane numbers (MON) are blend octane numbers acquired with 5% and 10% fuel blends. The basestock fuel was an oxygen free gasoline fuel with a RON of 82.4 and a MON of 76.6, respectively [1]. The octane ratings of the basestock fuel were lower compared to standard pump grade fuel. This led to a larger spread in octane number estimation of the blended fuels. A strong non-linear behaviour in blend octane number for RON is observed whereas the MON stays nearly constant.

Density[1] [kg/m^3]	BP [°C]	LHV [kJ/l]	Oxygen [%wt]	Blend	RON[2]	MON[2]
810	79.6	25250	22.2	5% 10%	102.4 108.4	99.6 100.6

Table 1 Physical properties of 2-butanone [1, 7, 8]
[1]reference temperature 20 °C
[2]from 5 % resp. 10 % blends with 82.4 RON and 76.6 MON basestock

The initial temperature of the fuel-air mixture inside the combustion vessel prior to ignition was set to 373 K and the initial mixture pressures were set to 1 atm and 5 bar. Experiments were conducted with equivalence ratios ranging between 0.7 and 1.3 in steps of 0.1. The sensitivity of the kinetic mechanism to temperature variations was checked with additional experimental points measured at a temperature of 423 K, with pressures of 1 atm and 5 bar, and equivalence ratios of 0.8 and 1.3.

CHEMICAL KINETIC MECHANISMS AND FLAME SPEED

The laminar flame speed calculations were performed using the 1D premixed, freely propagating flame module of the FlameMaster software package [9].

A kinetic model for the oxidation of 3-pentanone [10], consisting of 233 species and 1366 reactions, which also includes the 2-butanone submechansim [11], is used for the calculation of 2-butanone laminar burning velocities in the present work. The 3-pentanone mechanism is available online from the Combustion Chemistry Centre at NUI Galway [12]. The mechanism was validated against shock tube experiments for lean, stoichiometric, and rich conditions for acetone / oxygen mixtures and 3-pentanone / oxygen mixtures, both diluted with argon. Also, flame speed data under ambient conditions for acetone, 2-butanone, and 3-pentanone were used for validation of the mechanism [10, 11, 13].

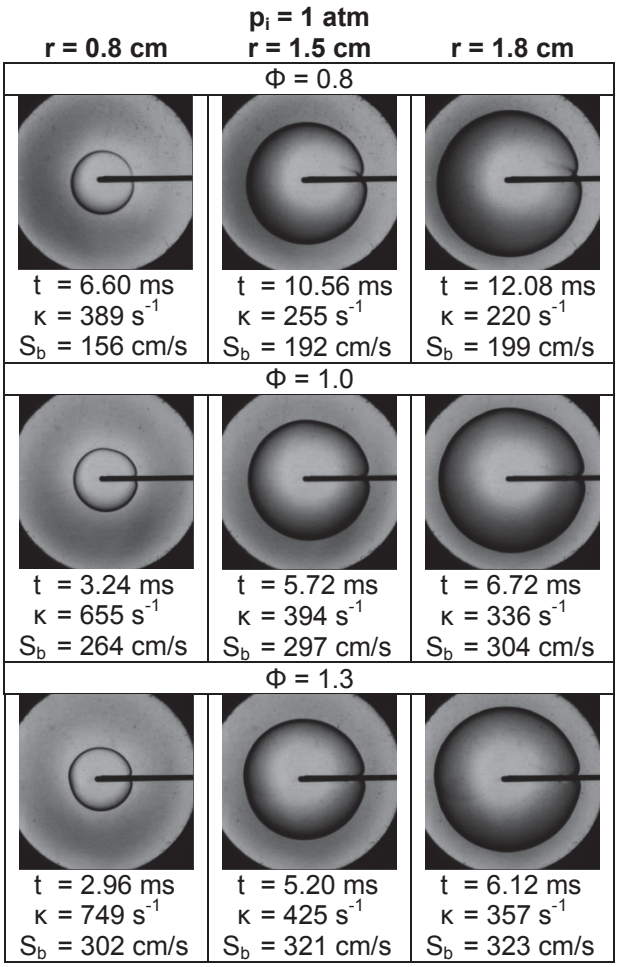

Figure 2 Captured images of spherical 2-butanone / air flames; Φ = 0.8, 1.0 and 1.3; p = 1 atm and T = 373 K

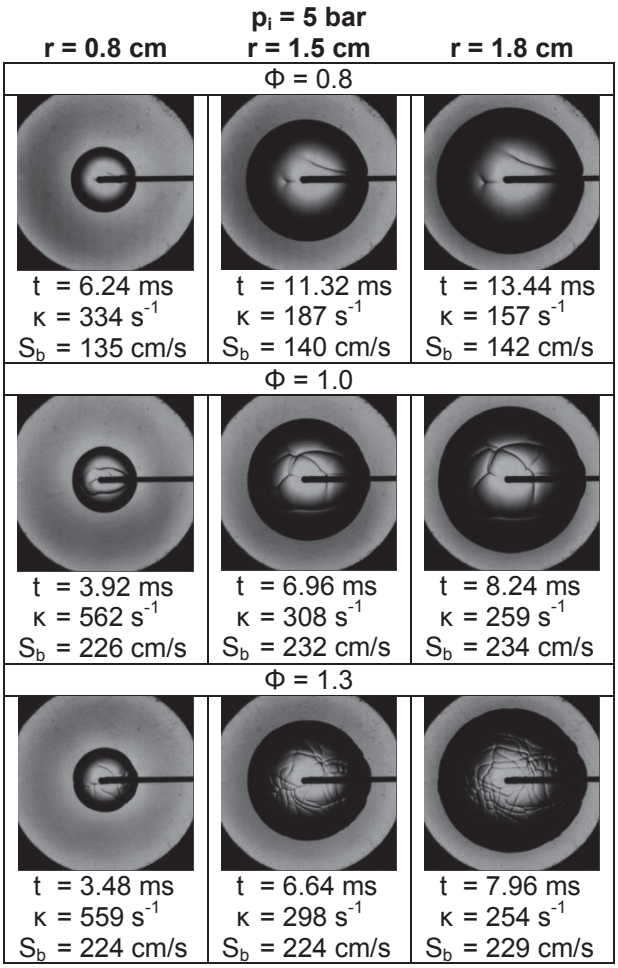

Figure 3 Captured images of spherical 2-butanone / air flames; Φ = 0.8, 1.0 and 1.3; p = 5 bar and T = 373 K

DETERMINATION OF FLAME SPEEDS

The evaluation of the observed experimental data was restricted to spherical smooth flame fronts with a radius above 7 mm in order to avoid the spark's influence as a result of the ignition process [14, 15, 16, 17]. The flame front was extracted from the captured Schlieren images using the method of Otsu et al. [18]. The image post-processing of the propagating flame, performed under the assumption of constant pressure, yields information of the expanding flame radius r_f over time t. The stretched propagation speed with respect to the burnt mixture S_b can then be determined by the derivative dr_f/dt applying a central difference scheme. The stretch rate κ is defined as the temporal change of a flame surface area A [19]. In case of a spherically outwardly expanding flame front, κ can be expressed as follows:

Eq. 1 $$\kappa = \frac{1}{A}\frac{dA}{dt} = \frac{2}{r_f}\frac{dr_f}{dt}.$$

The response of flames to stretch has been analysed on the basis of an asymptotic analysis by Clavin and Williams [20], Pelce and Clavin [21], and Matalon and Matkowsky [22]. It has been shown in [22, 23] that the burnt gas Markstein length L_b that expresses the influence of stretch on the flame speed can be described as

Eq. 2 $$S_b^0 - S_b = L_b\kappa,$$

where S_b^0 is the unstretched flame speed of the burnt mixture. The burnt flame speed is plotted against the stretch rate κ. A least-squares fit yields the unstretched flame speed S_b^0 and the Markstein length L_b.

In addition to the linear model from Eq. 2 a non-linear model was utilized to extract S_b^0 and L_b. This technique has been discussed by Halter et al. [24], which is based on an earlier work of Ronney and Sivashinsky [25] and is given by:

Eq. 3 $$\left(\frac{S_b}{S_b^0}\right)^2 \ln\left(\frac{S_b}{S_b^0}\right)^2 = -\frac{2L_b\kappa}{S_b^0}.$$

Again a least-squares fit is applied to obtain the unknows, S_b^0 and L_b.. As a result, the following expression is minimised:

Eq. 4 $$\sum_{i=m}^{N}\left|\left(\frac{S_b}{S_b^0}\right)^2 \ln\left(\frac{S_b}{S_b^0}\right)^2 + \frac{2L_b\kappa}{S_b^0}\right|,$$

where N corresponds to the number of discrete observation times. Kelly and Law [26, 27] proposed a more accurate method to solve for the two unknowns of Eq. 3 using an analytical solution based only on the temporal evolution of the flame radius, hereafter referred to as the non-linear method.

The laminar burning velocity S_L is defined as the unstretched flame displacement speed with respect to the unburnt mixture, S_u^0. In this study, it is determined from mass continuity through a planar unstretched flame

Eq. 5 $$S_L = S_u^0 = S_b^0 \left(\frac{\rho_b}{\rho_u}\right).$$

Here, ρ_b and ρ_u are the densities of the burnt and unburnt mixture. ρ_b is evaluated at adiabatic flame temperature conditions.

RESULTS AND DISCUSSION

In this section, the experimental results of the flame speed measurements are presented and discussed. First, images of spherical flames for 2-butanone / air mixtures are shown and described. On the basis of measured propagation speed over stretch, figures illustrating both the application of linear and non-linear extrapolation techniques, are shown. The differences in unstretched flame speeds as an outcome of the varying extrapolation techniques are highlighted. Also, reasons for the observed spreading are emphasised. Hereafter, the new experimental data and data taken from the literature are compared with calculated flame speeds. Images of the spherical flames of 2-butanone / air mixtures at equivalence ratios of 0.8, 1.0, and 1.3 are shown in Figure 2 and Figure 3. Images are taken at three different flame radius locations of 0.8 cm, 1.5 cm, and 1.8 cm. For both figures, the initial chamber temperature prior to ignition is set to 373 K. In Figure 2 the initial pressure is 1 atm and in Figure 3 it is 5 bar. In addition, flame radius r_f stretch κ, and corresponding flame propagation speed S_b are given. The elongated electrodes of the spark plug are positioned in the centre of the combustion vessel.

For the 1 atm measurements, the flame contour remains smooth throughout the entire visible flame radius evolution. In contrast, with increasing initial chamber pressure, small artefacts are visible on the flame surface resulting from the ignition process. For lean and stoichiometric mixtures, several consecutive runs were compared with each other in order to examine the influence of these artefacts on the flame speed evolution. The images varied from flames without any visible artefacts up to the amount of disturbances shown in Figure 3. The amount of visible artefacts does not significantly increase during the investigated flame radius evolution. Thus, the artefacts seem not to influence the resulting propagation speed.

For richer mixtures such as an equivalence ratio of 1.3, the number of cellular structures increases with increasing flame radii. The constraint of quasi isobaric conditions for post processing must also be taken into account. Thus, flame radii are used for extrapolations which do not show wrinkling of the flame contour nor cell splitting and which are quasi isobaric. Certainly, with richer mixtures as well as with increasing initial chamber pressure, the radius range of flame images acceptable for post processing is decreasing. The uses of argon instead of nitrogen for further dilution are suitable measures in order to suppress cellularities for a pressure and equivalence range extension.

In general, due to the lower propagation speed of lean mixtures, the evolution of the corresponding flame speeds is taking place at much lower stretch rates compared to the stoichiometric and rich mixtures. For example, in Figure 2 at a radius of 0.8 cm, the burnt flame speed of the lean mixture is 156 cm/s at a stretch rate of 389 s^{-1}, whereas the burnt propagation speed and the stretch rate have nearly doubled for the stoichiometric and rich mixtures.

This behaviour is also illustrated in Figure 4 and Figure 5, where the corresponding flame speed extractions over the stretch rate are shown at 373 K for 1 atm and 5 bar, respectively. The temporal evolution of the flame goes from high to low stretch values. Symbols indicate the results of the post-processed flame images. Solid lines represent the non-linear extrapolation according to Eq. 3 and dashed lines the linear extrapolation technique according to Eq. 2. The extrapolation has been applied while the chamber pressure remains nearly constant. The pressure rise limit for the post processing was set to less than 2.5%, with 2.5% for ambient pressure and 1.0% for 5 bar measurements. The pressure limit and hence the limit for extrapolation is marked for each measurement in Figure 4 and Figure 5 by a vertical dash with the corresponding flame radius r_p.

An exception has to be made when the influence of cellular structures on the flame surface area is appearing earlier than the limit due to pressure rise. The extrapolation of the data must be performed from the biggest flame radius usable in the set of measurements towards small, higher curved flames.

For the 1 atm measurements shown in Figure 4, the non-linear extrapolation nicely follows the flame speed evolution over stretch for lean to rich mixtures. Only for the rich case, marginal discrepancies for small, curved flames with stretch rates above 750 s^{-1} are noticeable. On the other hand, the linear extrapolation routine cannot be applied for equivalence ratios leaner than Φ = 1.1, simply because there is no region of linear flame speed over stretch evolution. For an equivalence ratio of 0.8, for instance, a small data range from stretch rates of 350 s^{-1} to the point of 2.5 % pressure increase might be identified for extrapolation. This region, still slightly curved, leads to linearly extrapolated planar flame

speeds too fast. The data range with a linear evolution of flame speed over stretch which is applicable for linear extrapolation increases with equivalence ratios higher than 1.0. Furthermore, asymptotic analysis, based on weakly stretched flames, encourages the use of the linear extrapolation, once an adequate number of linear data points are available.

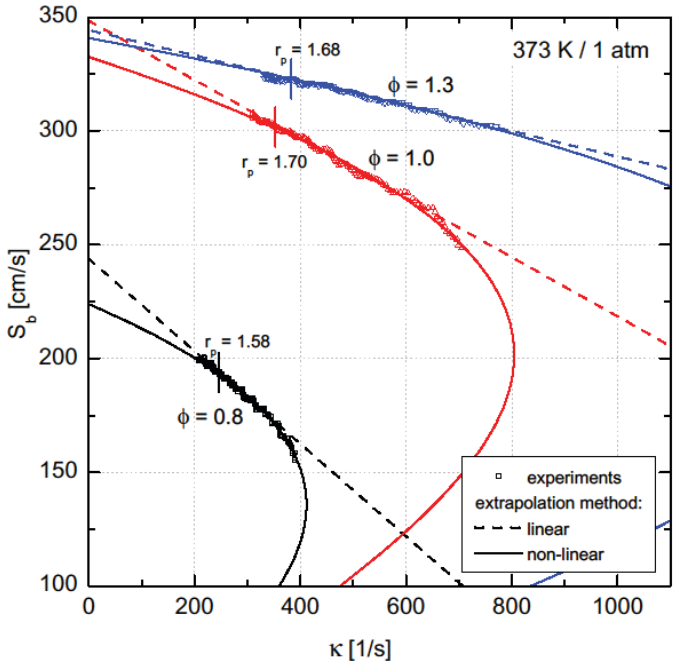

Figure 4 Measured flame propagation speed over stretch for 2-butanone / air flames; equivalence ratios of 0.8, 1.0 and 1.3; p = 1 atm and T = 373 K; linear and non-linear extrapolation

For an increased initial pressure of 5 bar, as shown in Figure 5, the linear and non-linear extrapolations yield nearly identical results for lean to stoichiometric mixtures with positive Markstein lengths. But then, for a rich mixture of Φ = 1.3 the flame speed over stretch evolution yields a negative Markstein length. Still, the linear extrapolation follows perfectly the experimental data. However, the non-linear extrapolation fails to fit correctly the experiments giving incorrect flame speeds and Markstein length. Data of the Markstein lengths and the unstretched flame speed in the burnt mixture for linear and non-linear extrapolation at the investigated experimental conditions are given for completeness in Tables 2 and 2 of the Appendix.

One also has to take into account, when extrapolating the data, that a sharp kink in flame speed over stretch can be observed with increasing equivalence ratio at lower stretch rates, which is due to the formation of cellular structures (see also Figure 3, equivalence ratio of 1.3 at radii of 1.5 and 1.8 cm). This is due to the transition from stable to cellular flames. In general, the influence of instabilities on the flame speed is identified by a particularly sharp increase in flame speed as flame stretch decreases [16]. The earlier onset of the formation of cellular structures as a result of richer mixtures and increasing initial pressure in combination with the radius restriction due to the ignition process of 7 mm limits the range of accurately determined laminar flame speeds to flames with an equivalence ratio up to 1.3. This limit must be carefully checked depending on the fuel used, initial temperature, and pressure. Also buoyancy may affect the results and must be thoroughly checked. This can be achieved by tracking the position of the centre of the spherical flame over time.

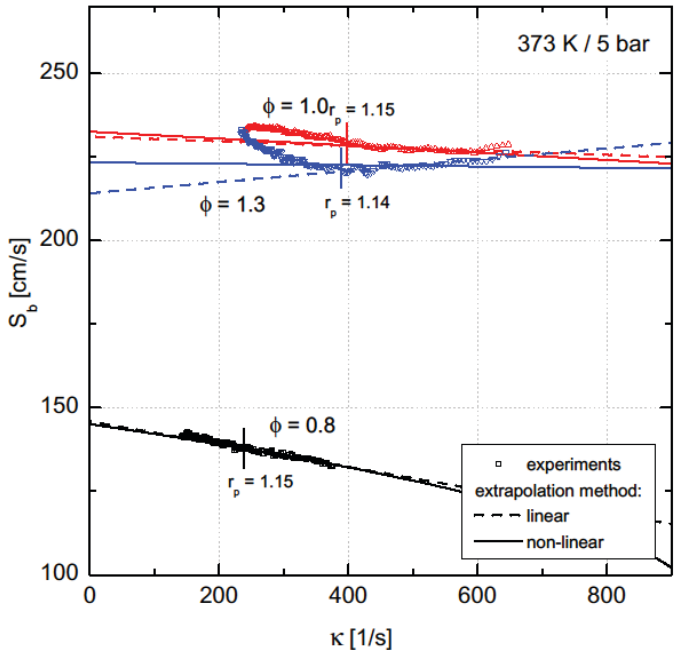

Figure 5 Measured flame propagation speed over stretch for 2-butanone / air flames; equivalence ratios of 0.8, 1.0 and 1.3; p = 5 bar and T = 373 K; linear and non-linear extrapolation

Figure 6 and Figure 7 present the laminar burning velocity results of this study for both the linear and the non-linear extrapolation. Both figures also show the utilised and the refused data points of the extrapolation process in order to highlight possible error sources. Figure 6 shows the new experimental data for 373 K and 423 K at atmospheric pressure. As an outcome from the previous discussion, the non-linear extrapolation is found to be applicable for lean to stoichiometric mixtures. Maximum flame speed for 373 K is found at an equivalence ratio of around 1.2, which also corresponds to the maximum position of the computed flame speeds. For equivalence ratios of 1.1 to 1.3, linear extrapolation is utilised.

Calculated flame speeds underpredict stoichiometric to lean mixtures and marginally overpredict rich mixtures. For a higher temperature of 423 K, the simulation clearly underpredicts the lean and overpredicts the rich reference cases, indicating a lack in temperature sensitivity of the chemical mechanism.

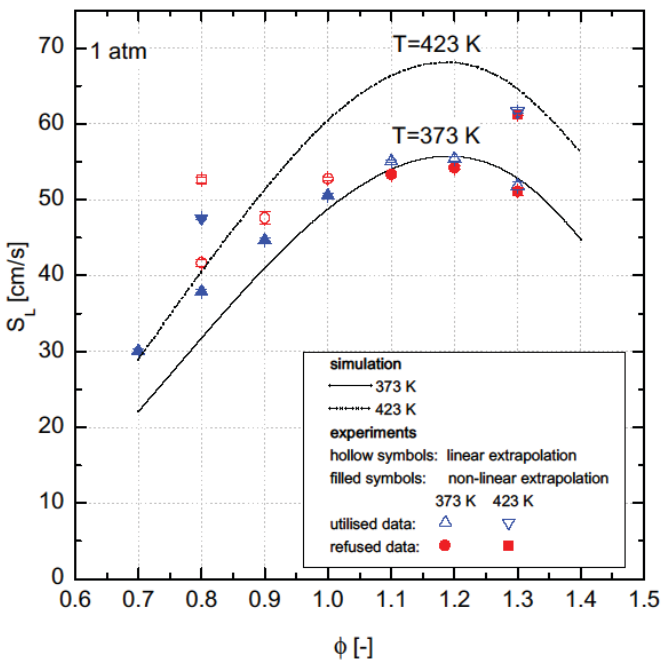

Figure 6 Experiments and simulations of laminar burning velocities for 2-butanone / air flames as a function of equivalence ratio; p_i = 1 atm and T_i = 373 K and 423 K

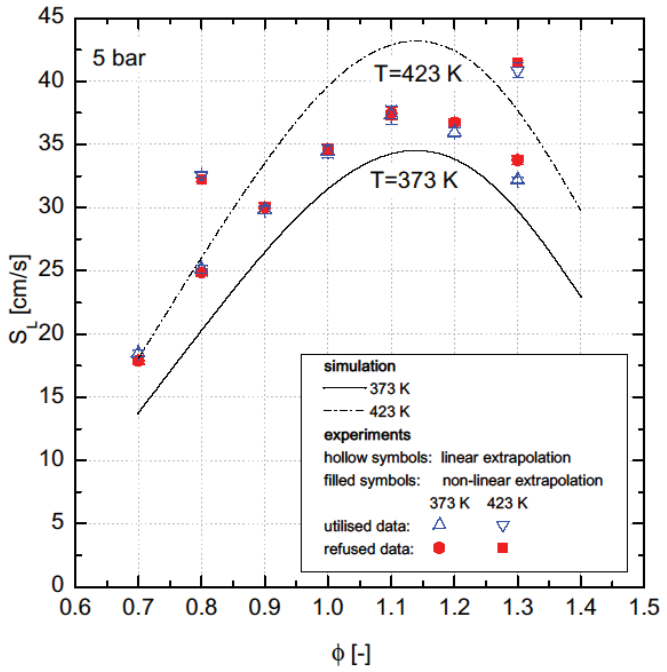

Figure 7 Experiments and simulations of laminar burning velocities for 2-butanone / air flames as a function of equivalence ratio; p_i = 5 bar and T_i = 373 K and 423 K

The 5 bar experimental data and corresponding simulations are given in Figure 7, again for temperatures of 373 K and 423 K. From lean up to mixtures with an equivalence ratio of 1.1, the data for the linear and the non-linear extrapolation nearly coincide. For richer cases than Φ = 1.1, the linear results have to be exclusively taken. This is due to the fact that the non-linear extrapolation fails to correctly fit the experimental data for negative Markstein length. For example, the linear result for Φ = 1.3 corresponds to 32.3 cm/s and to 33.8 cm/s for the non-linear result.

Comparing now the experimental data with the computed, the simulation clearly underpredicts the experiments over the entire equivalence ratio range. This indicates not only that the mechanism fails to predict correctly temperature sensitivity but also fails to predict correctly the pressure sensitivity. At a temperature of 423 K, again, the simulation clearly underpredicts the data at equivalence ratios of 0.8 and 1.3.

CONCLUDING REMARKS

Laminar burning velocities have been measured for 2-butanone in a spherical combustion vessel. The unburnt gas conditions were 1 atm and 5 bars at temperatures of 373 K and 423 K. The experimental results are presented in comparison with computed flame speeds by a 3-pentanone mechanism including a 2-butanone submechanism. The computed values fail to predict correctly the experiments by generally underpredicting burning velocities for lean mixtures. For rich conditions, the simulations partly overpredict at atmospheric pressure and underpredict for increasing pressure. The reason for this could have its origin in an incorrect sensitivity of the mechanism to pressure as well as to temperature variations. The acquired data has been post-processed to obtain the flame speed and the stretch rate of the propagating spherical flames. A linear and a non-linear extrapolation technique has been utilised to obtain the unstretched laminar flame speed. Both extrapolation procedures have been compared with each other under the assumption of constant vessel pressure. Three regions for the use of the individual extrapolation routine are identified. In the first region, only non-linear extrapolation is possible due to a lacking linear region for the acquired radius data range of the spherical flames (e.g.: lean to stoichiometric mixtures at ambient pressure). In the second region, both extrapolation techniques yield results which differ marginally from each other (e.g. lean to stoichiometric mixtures at 5 bar). Thus, both can be used equally. According to the asymptotic analysis of laminar flames, a linear extrapolation is favoured. In the third region (e.g. rich mixtures at increased pressures), only the linear extrapolation technique should be applied. The experimental data, yielding negative Marktein length, is not fitted correctly by the non-linear extrapolation routine. It is strongly recommended to always carefully assess the right extrapolation technique for different experimental conditions such as temperature, pressure, and equivalence ratio.

ACKMOWLEDGMENTS

This work was performed as part of the Cluster of Excellence "Tailor-Made Fuels from Biomass", which is funded by the Excellence Initiative of the German federal and state governments to promote science and research at German universities.

CONTACT

Joachim Beeckmann
Institute for Combustion Technology
RWTH Aachen University
Templergraben 64, 52056 Aachen, Germany
E-Mail: jbeeckmann@itv.rwth-aachen.de

REFERENCES

[1] C. Spindelbalker and A. Schmidt. Sauerstohaltige kraftstoffextender. Erdoel, Erdgas, Kohle, 10:469-474, 1986.

[2] J. Beeckmann, L. Cai, and H. Pitsch. Experimental investigation of the laminar burning velocities of methanol, ethanol, n-propanol, and n-butanol at high pressure. Fuel, 117, Part A(0):340-350, 2014.

[3] Gary S. Settles. Schlieren and Shadowgraph Techniques: Visualizing Phenomena in Transparent Media, volume 2. Springer Berlin, 2001.

[4] Luminus Devices, Inc. CBT-120 Product Datasheet, 2011.

[5] B. Poling, J. Prausnitz, and J.O. Connell. The Properties of Gases and Liquids. McGraw Hill professional. McGraw-Hill, 2000.

[6] J. Beeckmann, N. Chaumeix, P. Dagaut, G. Dayma, F. Foucher, F. Halter, A. Lefebvre, C. Mounaim-Rousselle, H. Pitsch, B. Renou, and E. Varea. Collobartive study for accurate measurements of laminar burning velocity. 6th European Combustion Meeting, Lund, Sweden, 2013.

[7] NIST Chemistry WebBook 2-butanone. http://webbook.nist.gov/cgi/cbook.cgi?ID=78-93. National Institute of Standards and Technology.

[8] GESTIS Substance Database for 2-butanone. http://gestis-en.itrust.de/nxt/gateway.dll?f=templates$fn=default.htm$vid=gestiseng:sdbeng.

[9] H. Pitsch. Flamemaster: A C++ computer program for 0D combustion and 1D laminar flame calculations.1998.

[10] Z. Serinyel, N. Chaumeix, G. Black, J.M. Simmie, and H.J. Curran. Experimental and chemical kinetic modeling study of 3-pentanone oxidation. The Journal of Physical Chemistry A, 114(46):12176-12186, 2010.

[11] Z. Serinyel, G. Black, H.J. Curran, and J.M. Simmie. A shock tube and chemical kinetic modeling study of methy ethyl ketone oxidation. Combustion Science and Technology, 182(4-6):574-587, 2010.

[12] 3-pentanone mechansim NUI Galway. http://c3.nuigalway.ie/3pentanone.html.

[13] S. Pichon, G. Black, N. Chaumeix, M. Yahyaoui, J.M. Simmie, H.J. Curran, and R. Donohue. The combustion chemistry of a fuel tracer: Measured flame speeds and ignition delays and a detailed chemical kinetic model for the oxidation of acetone. Combustion and Flame, 156(2):494-504, 2009.

[14] Z. Chen, M.P. Burke, and Y. Ju. Effects of Lewis number and ignition energy on the determination of laminar flame speed using propagating spherical flames. Proceedings of the Combustion Institute, 32(1):1253-1260, 2009.

[15] D. Bradley, P.H. Gaskell, and X.J. Gu. Burning velocities, Markstein lengths, and flame quenching for spherical methane-air flames: a computational study. Combustion and Flame, 104(1):176-198, 1996.

[16] D. Bradley, R.A. Hicks, M. Lawes, C.G.W. Sheppard, and R. Woolley. The measurement of laminar burning velocities and Markstein numbers for iso-octane-air and iso-octane-n-heptane-air mixtures at elevated temperatures and pressures in an explosion bomb. Combustion and Flame, 115(1):126-144, 1998.

[17] A. Y. Starikovskii. Plasma supported Combustion. Proceedings of the Combustion Institute, 30(2):2405-2417, 2005.

[18] N. Otsu. A threshold selection method from gray-level histograms. IEEE transaction on systems and cybernetics, 9(1):62-66, 1979.

[19] F.A. Williams. Combustion theory : the fundamental theory of chemically reacting flow systems. Combustion Science and Engineering Series. Menlo Park, Calif. Benjamin/Cummings Pub. Co. c1985, 1985.

[20] P. Clavin and F.A. Williams. Effects of molecular diffusion and of thermal expansion on the structure and dynamics of premixed flames in turbulent flows of large scale and low intensity. Journal of Fluid Mechanics, 116:251-282, 1982.

[21] P. Pelce and P. Clavin. Influence of hydrodynamics and diffusion upon the stability limits of laminar premixed flames. Journal of Fluid Mechanics, 124:219-237, 1982.

[22] M. Matalon and B.J. Matkowsky. Flames as

gasdynamic discontinuities. Journal of Fluid Mechanics, 124:239-259, 1982.

[23] C.K. Wu and C.K. Law. On the determination of laminar flame speeds from stretched flames. Symposium (International) on Combustion, 20(1):1941-1949, 1985.

[24] F. Halter, T. Tahtouh, and C. Mounaim-Rousselle, Nonlinear effects of stretch on the flame front propagation. Combustion and Flame, 157(10):1825-1832, 2010.

[25] P.D. Ronney and G.I. Sivashinsky. A theoretical study of propagation and extinction of nonsteady spherical flame fronts. SIAM Journal on Applied Mathematics, 49(4):1029-1046, 1989.

[26] A.P. Kelley and C.K. Law. Nonlinear effects in the experimental determination of laminar flame properties from stretched flames. In Fall technical meeting: eastern states sections of the Combustion Institute, Virginia, paper B-11, 2007.

[27] A.P. Kelley and C.K. Law. Nonlinear effects in the extraction of laminar flame speeds from expanding spherical flames. Combustion and Flame, 156(9):1844-1851, 2009.

APPENDIX

373 K								
1 atm								
		0.7	**0.8**	**0.9**	**1.0**	**1.1**	**1.2**	**1.3**
LM[1]	L_b [cm]		0.212	0.160	0.128	0.102	0.081	0.059
	S_b^0 [cm/s]		245.5	292.4	346.6	369.2	370.7	344.7
NM[2]	L_b [cm]	0.147	0.099	0.082	0.076	0.066	0.057	0.044
	S_b^0 [cm/s]	162.7	222.8	272.1	331.5	357.9	363.1	339.9
5 bar								
LM[1]	L_b [cm]	0.064	0.035	0.008	0.007	0.001	-0.008	-0.019
	S_b^0 [cm/s]	100.2	148.7	189.2	230.2	249.40	241.9	213.75
NM[2]	L_b [cm]	0.041	0.027	0.011	0.009	0.005	0.002	0.002
	S_b^0 [cm/s]	97.2	147.1	190.8	231.4	251.7	247.1	224.2

Table 2 Markstein lengths and unstretched flame speed in the burnt for linear and non-linear extrapolation; equivalence ratios between 0.7 and 1.3; p = 1 atm and 5 bar; T = 373 K

[1]linear extrapolation technique

[2]non-linear extrapolation technique

423 K					
		1 atm		5 bar	
		0.8	1.3	0.8	1.3
LM[1]	L_b [cm]	0.193	0.052	0.95	-0.004
	S_b^0 [cm/s]	277.8	365.8	172.6	243.1
NM[2]	L_b [cm]	0.091	0.043	0.031	0.002
	S_b^0 [cm/s]	252.5	363.5	170.7	246.6

Table 3 Markstein lengths and unstretched flame speed in the burnt for linear and non-linear extrapolation; equivalence ratios of 0.8 and 1.3; p = 1 atm and 5 bar; T = 423 K
[1]linear extrapolation technique
[2]non-linear extrapolation technique

The Engineering Meetings Board has approved this paper for publication. It has successfully completed SAE's peer review process under the supervision of the session organizer. This process requires a minimum of three (3) reviews by industry experts.

ISSN 0148-7191